LA-UR- 97-4967

Title: **Measurement of Point Defect Energetics in Potassium Dihydrogen Phosphate (KDP)**

Author(s): **D. W. Cooke, R. E. Muenchausen and B. L. Bennett**

Submitted to: **Informal Report**

Los Alamos
NATIONAL LABORATORY

Form No. 836 R5
ST 2629 10/91

DISCLAIMER

MEASUREMENT OF POINT DEFECT ENERGETICS IN POTASSIUM DIHYDROGEN PHOSPHATE (KDP)

D. Wayne Cooke
LANL, MST-8, MS E546, 505-667-4274 [cooke@lanl.gov]

Ross E. Muenchausen
LANL, MST-11, MS D429, 505-667-0391 [rossm@lanl.gov]

Bryan L. Bennett
LANL, MST-8, MS E546, 505-667-3640 [b_bennett@lanl.gov]

FINAL REPORT

Prepared for
Jim De Yoreo and Ming Yan
Lawrence Livermore National Laboratory

October 17, 1997

1. INTRODUCTION

Potassium dihydrogen phosphate (KDP) in the normal and deuterated form (KD*P) exhibits excellent electrooptical and nonlinear optical properties and is commonly used in frequency conversion applications [Y. Xu, in Ferroelectric Materials and Their Applications (North Holland, Amsterdam, 1991)]. Frequency doubling (2ω) of Nd:YAG or Nd:YLF laser fundamental output at 1.06 μm produces visible radiation at 532 nm with relatively good conversion efficiency. Frequency tripling (3ω) and quadrupling (4ω) are also utilized for production of ultraviolet (*uv*) radiation at 355 and 266 nm, respectively. However in the latter case the conversion efficiency is relatively low, especially at high incident fluences (~ 2 GW/cm^2). A fundamental problem associated with high peak-power laser excitation of KDP is the production of transient optical absorption that inhibits conversion efficiency.

Various mechanisms have been postulated to account for the low conversion efficiency, including unusually large 4ω two-photon absorption coefficients [G. J. Linford *et al.*, *Appl. Opt.* **21**, 3633 (191982)], and broad *uv*-induced transient absorption [J. E. Davis *et al.*, *Chem. Phys. Lett.* **207**, 540 (1993)]. According to Davis *et al.*, the transient electronic defects in KDP are formed at room temperature within 2 ps after *uv* two-photon excitation, and decay nonexponentially in ca. 20 s. The measured transient absorption spectrum covers the spectral region from approximately 300 to 700 nm and is independent of host impurity content. From time-resolved pump-probe defect decay dynamics, Davis *et al.* suggested that diffusive transport of a proton or hydrogen atom in KDP and a deuteron or deuterium in KD*P were responsible for the decay of the absorption. Electron spin resonance (ESR) studies have indeed identified a hydrogen defect in KDP following exposure to *x*-ray, *e*-beam, or γ radiation at 77 K [K. Tsuchida and R. Abe, *J. Phys. Soc. Japan* **38**, 1687 (1975)]. This defect (labeled "Defect A" in the literature) has been identified as a hydrogen deficient phosphate radical ion $HPO^{\bullet}_4^-$ which possibly results from electron-hole production via two-photon absorption and subsequent hole capture at an O-H bond with concomitant ejection of a proton. Davis *et al.*, hypothesized that transient defects are created by two-photon absorption and simultaneously bleached by the *uv* beam. Based on the similarity of the spectral dependence of the transient absorption band and a previously reported *x*-ray induced band [E. Dieguez and J. M. Cabrera, *J. Phys. D* **14**, 91 (1981)] it was suggested that the defects are intrinsic to KDP and are associated with the $HPO^{\bullet}_4^-$ radical (Defect A) with formation and decay mechanisms based on protonic transport within the hydrogen bond network of $H_2PO_4^-$ ions. Experimental evidence supporting this view has recently been presented by Setzler, *et al.* [S. D. Setzler, K. T. Stevens, L. E. Halliburton, M. Yan, N. P. Zaitseva,

and J. J. De Yoreo, *Phys. Rev. B*, preprint] wherein they report direct observation of hydrogen atoms in KDP induced at 77 K by either *x* rays or 266-nm photons. The atoms occupy interstitial sites and, along with the well-known $HPO^{\bullet}_4^-$ radicals (hole centers), thermally decay between 80 and 200 K. An important conclusion of this work is that impurities or other point defects are not required to act as precursors for hydrogen atom and hole center formation thereby implying that transient optical absorption is an *intrinsic* phenomenon which occurs in pure KDP.

Combined optical absorption and ESR studies [J. A. McMillan and J. M. Clemens, *J. Chem. Phys.* **68**, 3627 (1978)] have led investigators to suggest that a second defect (labeled "Defect B" in the literature) exists in KD*P and is believed to be a $H_2PO^{\bullet}_4$ neutral radical. Davis *et al.*, concluded that Defect B is either not formed at room temperature or decays too quickly to be observed and, therefore, is not associated with the broad transient absorption observed in KDP.

A quantitative analysis of the effect of *uv*-induced transient absorption on frequency conversion in KDP has been given by Marshall *et al.* [C. D. Marshall, *et al.*, *J. Opt. Soc. Am. B* **11**, 774 (1994)]. In addition to measuring the transient absorption spectrum they investigated transient absorption decay times of seven different KDP crystals, five different KD*P specimens, one rubidium dihydrogen phosphate sample and one ammonium dihydrogen phosphate crystal. Remarkably, the decay times varied by more than six orders of magnitude (0.2 to 4 x 10^5 s) although the peak absorption strengths at zero time delay were indistinguishable for crystals under the same excitation conditions. Furthermore it was concluded that the purest crystal (*i.e.*, the one with the least concentration of dislocations and impurities) exhibited the longest transient absorption decay time.

The role of point defects on frequency conversion efficiency and optoelectronic device performance in KDP and its isomorphs is not fully understood. However, it is evident from the extant data that their existence, even in pure specimens, affects the overall performance of these technologically important materials, and that further research is required to elucidate their role. Accordingly, we have investigated the temperature-dependent optical absorption and radioluminescence (RL) of pure KDP as well as doped specimens: KDP:Fe, KDP:Cr, and KDP:Al.

2. EXPERIMENTAL ASPECTS

A. Sample Description

The KDP crystals used in this investigation were grown at LLNL by the fast growth technique. Dimensions of the polished specimens ranged from 6 x 8 x 1 mm^3 to 10

x 10 x 1 mm^3 and were designated by LLNL as: KDP high purity (#63), KDP:Fe (#147), KDP:Cr (#181), and KDP:Al (#131). Dopant concentrations of the individual specimens as determined by LLNL were: 5 ppm Fe, 3 - 5 ppm Cr, and 3 ppm Al. The *c*-axis of each sample was along the short dimension

KDP has a noncentrosymmetric tetragonal point group 42*m* structure at room temperature and is therefore piezoelectric but not ferroelectric. As the temperature decreases below room temperature, KDP changes into a ferroelectric phase (first-order transition) with orthorhombic structure (point group *mm*2) at the Curie temperature (T_c = 123 K). The spontaneous polarization is caused by displacements of K^+, P^{5+} and O^{2-} ions along the direction of the *c*-axis in the tetragonal cell. The structural framework of KDP is composed of two interpenetrating sets of body-centered sublattice of PO_4 tetrahedra and of two interpenetrating sets of body-centered sublattice of K^+ ions. The K^+ ions and P^{5+} ions are alternately arranged in different layers, which are perpendicular to the *c*-axis and spaced apart by 1/4 *c*. Each phosphorous ion is surrounded by four oxygen ions at the corners of a tetrahedron. Each PO_4 group is linked to four other PO_4 groups, spaced 1/4 *c* apart along the *c*-axis, by hydrogen bonds. The linkage is such that there is an O–H–O hydrogen bond between one upper oxygen of one PO_4 group and one lower oxygen of the neighboring PO_4 group. Each hydrogen bond lies very nearly perpendicular to the *c*-axis. Neutron diffraction studies show that only two hydrogen atoms are located nearest to each PO_4 group and thus as a group they form $(H_2PO_4)^-$ ions. Moreover, the hydrogen atoms are statistically distributed at the center of O–H–O hydrogen bonds when the temperature is above T_c, but are statistically off center by about 0.35Å for temperatures below T_c.

B. Optical Absorption

A Cary 5E spectrophotometer was used to measure optical absorption of the KDP crystals. The sample chamber was modified to allow insertion of a temperature-controlled continuous-flow liquid-helium cryostat so that temperature-dependent absorption measurements could be made. Effects of the cryostat's quartz windows on the optical transmission of each sample was ascertained by first measuring its transmission in air at room temperature and comparing the result with the transmission measured in the cryostat at both ambient pressure and 10^{-6} Torr. The maximum difference was less than 1%. In a similar experiment comparison of the transmission at room temperature (in vacuum) with that obtained at 11 K was made to determine the effects of thermal contraction on the apparatus; the maximum difference was about 2%. Optical absorption of each sample was measured along the *c*-axis.

A typical optical absorption experiment included measuring optical transmission of the sample at room temperature, cooling to 11 K and recording the transmission again, followed by *x*-ray excitation and another transmission measurement. Subsequently, the temperature was raised at a nonlinear rate to values of 50, 100, 150, 250 and 295 K for additional transmission measurements. Each of these temperatures was maintained for about 5 minutes to allow thermal equilibration, after which time the optical transmission was measured in the interval 200 to 700 nm. Total measurement time at each temperature was about 20 min. Using a LakeShore temperature controller each stated temperature was maintained to an accuracy of ±1 K. Raw data were recorded as optical transmission and converted to absorbance for display [$A = \log_{10}(1/T)$].

All samples were given the same x-ray exposure at 11 K, 1 MR in air, at a rate of 200 R/s with a target-to-sample distance of 3.3 cm. X-rays emanated from a molybdenum target operating at 50 kV and 40 mA with a 25 keV effective energy, as measured by the half-value layer method. The cryostat was equipped with opposing quartz windows and a beryllium window to allow x-ray entry. Optical absorption experiments on the empty cryostat demonstrated that no measurable radiation damage occurred to the quartz windows during x-ray exposure.

C. Radioluminescence

Temperature-dependent radioluminescence (RL) of each KDP sample was obtained by cooling the specimen to 11 K and, under continuous *x*-ray excitation, detecting the resulting emission at various fixed temperatures. Light emanating from the sample was collected by a fiber optic cable, transmitted to the entrance slit of a 1/4-m monochromator, and detected by a cooled CCD camera. The system comprises an optical multichannel analyzer (OMA) that collects data in the interval 300 to 800 nm in 33 ms. An integration time of 6 min. was used in all RL measurements. Background spectra were accumulated for each experiment and subtracted from the raw data prior to presentation. Utilizing the known spectrum of a NIST-traceable tungsten lamp, nonlinearities in the spectral response of the OMA system were corrected. Second-order spectra from some specimens were observed and, because it was well defined, no effort was made to eliminate it from the raw data.

Irradiation of the samples occurred only after each fixed temperature was attained and stabilized. The total exposure for each specimen depended upon the number of RL data points but typically did not exceed 42 minutes (5.04×10^5 R).

3. RESULTS AND DISCUSSION

A. Optical Absorption

Shown in Fig. 1. are the optical absorption curves for the four KDP specimens measured at room temperature in the as-received state. All are relatively transparent above about 350 nm and each exhibit a well-defined absorption band near 275 nm. In the case of KDP:Fe there is also indication of a band near 215 nm. Except for KDP:Fe, the specimens show increasing absorption at our lowest measured wavelength (200 nm). KDP:Cr absorption reaches a value of 1.35 at 200 nm (not shown in Fig. 1). Dieguez and Cabrera [*J. Phys. D* **14**, 91 (1981)] have observed overlapping bands in unirradiated KDP at 215 and 280 nm and indicated that they extend beyond their detection limits (195 nm). It is now generally accepted that unirradiated KDP has an absorption band near 275 nm whose intensity depends upon dopant concentration. This band is well above the KDP fundamental absorption edge at 155 nm and is believed to be associated with "proton" vacancies, *i.e.*, an ion that has lost one proton from the normal H_2PO^{4-} lattice [proton vacancy = $(HPO_4)^{2-}$].

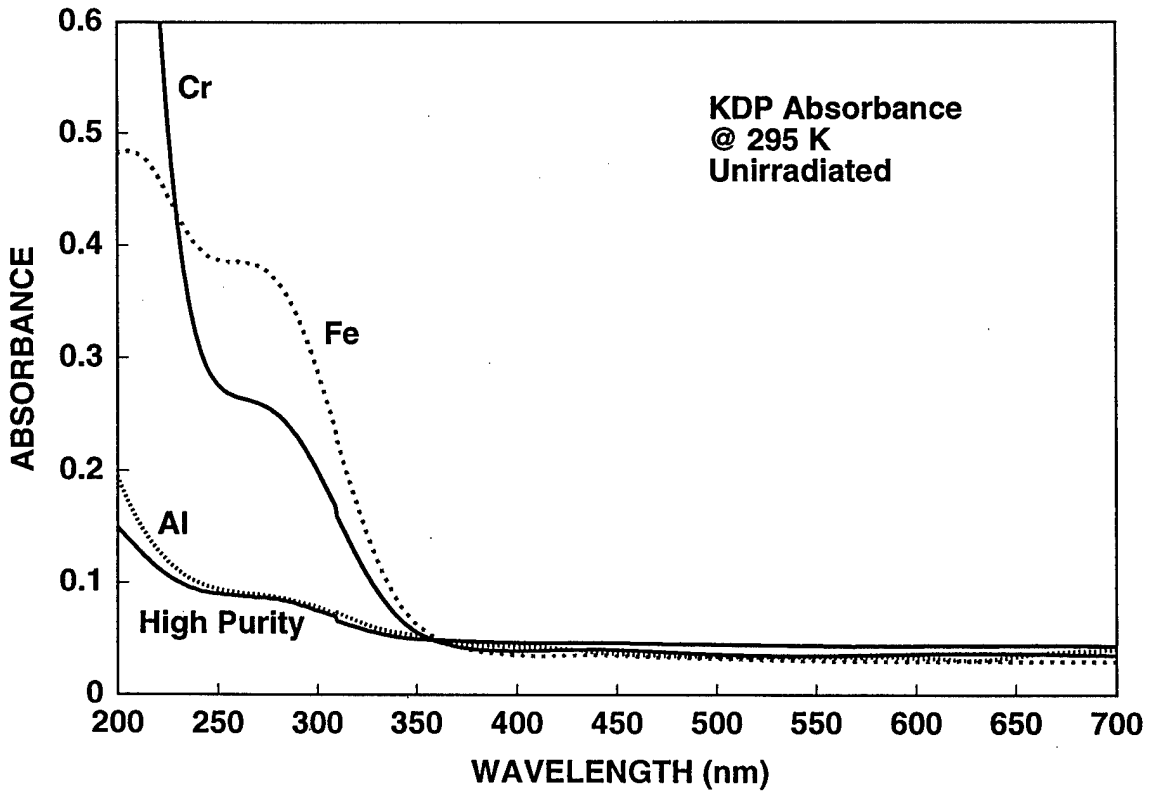

Fig. 1. Optical absorption of as-received high purity and doped KDP samples measured at room temperature.

This assignment is consistent with the data of Fig. 1 wherein the addition of metal (M) impurities, with the exception of Al, show an enhanced absorption at 275 nm. Assuming M^{3+} substitutes for K^{+} we expect two proton vacancies for charge compensation and, therefore, expect the doped specimens to exhibit enhanced absorption at 275 nm as observed. These data support earlier conclusions that the spectral position of this "intrinsic" defect is independent of the type of metal impurity, and the intensity depends only upon the total impurity concentration. Based on the work of Marshall *et al.* we certainly expect these specimens to contain other impurities at reduced concentration. The proton vacancy defect is diamagnetic and would not exhibit an ESR signature, consistent with the observation that ESR signals are absent in unirradiated KDP and KD*P (Setzler *et al.*).

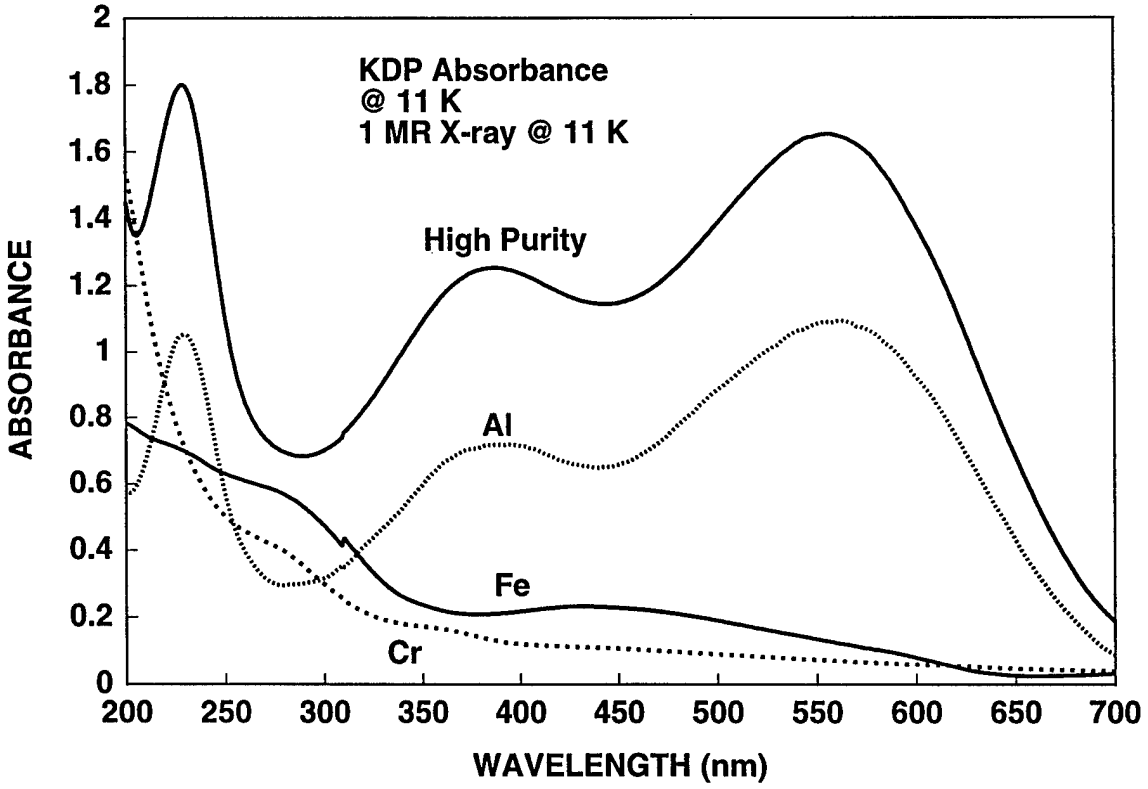

Fig. 2. Optical absorption of four KDP specimens *x* irradiated at 11 K.

As previously stated, there are no measurable differences between room temperature- and 11 K- optical absorption of the *unirradiated* samples. However, *x*-ray excitation at 11 K induces significant absorption in each sample, especially the high-purity and Al-doped specimens as shown in Fig. 2. Diéguez et al. [E. Diéguez, C. Zaldo, J. M. Cabrera and F. Agulló-López, *Induced Defects in Insulators*, 221 (19??)] have investigated optical absorption of metal-doped KDP specimens and found no evidence for radiation-induced absorption at room temperature. We assume that our samples behave accordingly.

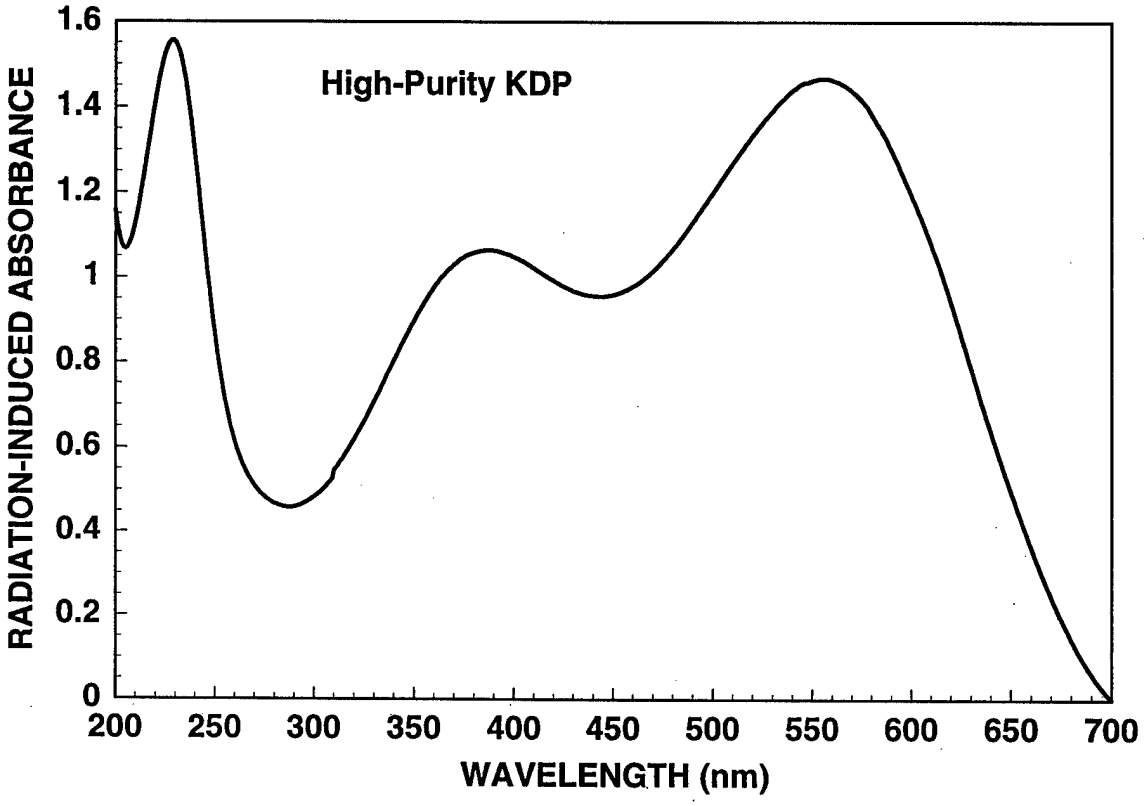

Fig. 3. Radiation-induced absorption of high-purity KDP measured at 11 K.

A striking feature of the data in Fig. 2 is the large radiation-induced absorption at 11 K in high purity and Al specimens as compared to the Fe and Cr samples. For example, the increase in absorption at 200 nm due to radiation of the former specimens is approximately an order-of-magnitude, considerably larger than that observed in Fe and Cr. Surprisingly, the Al-doped sample behaves similarly to the pure specimen although its impurity content is presumed to be similar to that of the Fe and Cr samples. Three

radiation-induced peaks with maxima near 225, 385 and 550 nm are clearly resolved in the absorption spectra of high purity and Al-doped KDP.

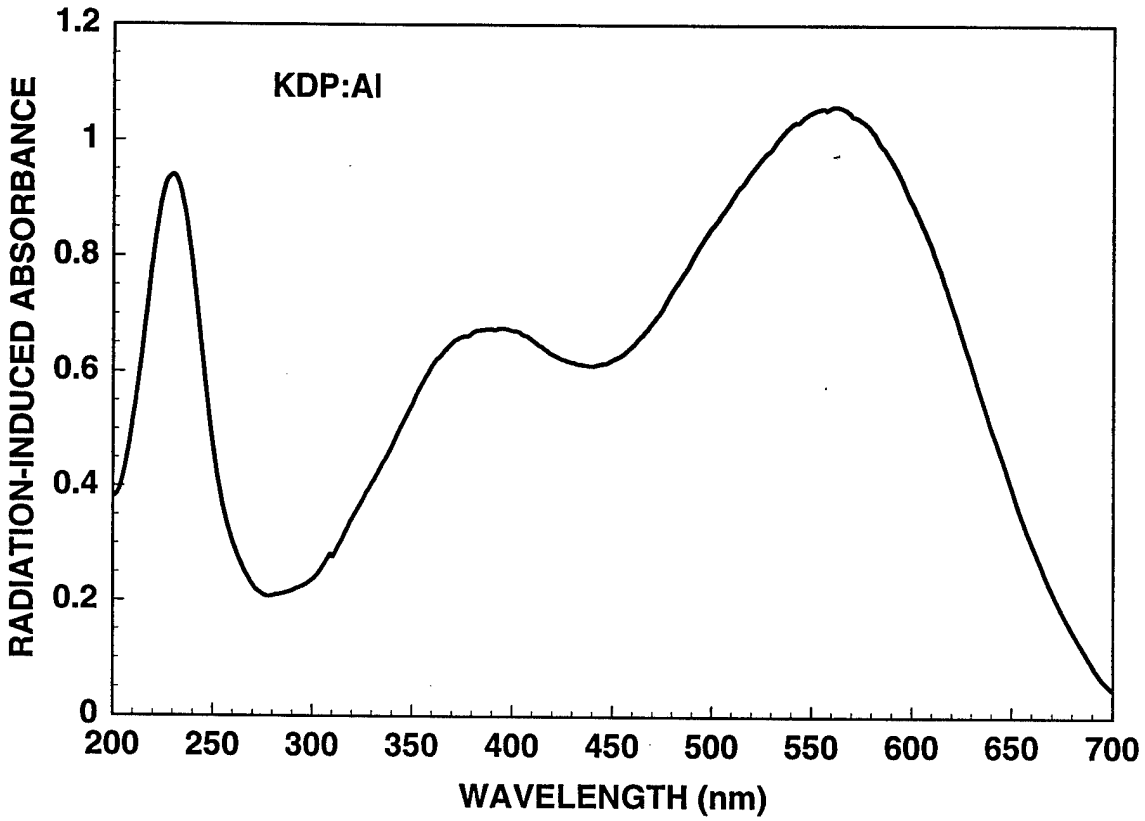

Fig. 4. Radiation-induced absorption of KDP:Al measured at 11 K.

In Figs. 3 and 4 we show the radiation-induced absorption obtained by subtracting the unirradiated from the irradiated values measured at 11 K. In addition to the prominent bands located at 385 and 550 nm there is a strong band with maximum near 225 nm. This band appears in each of the four irradiated absorption spectra and is not attributable to a shift of the 275-nm band that is observed in the unirradiated specimens. The absorption intensity of the 225- and 385-nm bands in high purity and Al-doped KDP precludes resolution of the 275-nm band; however, it is resolvable in the Fe- and Cr-doped samples, as shown in Figs 5 and 6. The thermal annealing behavior of each of the four specimens, which will be discussed later, clearly shows the evolution of the 225- and 275-nm peaks as the temperature increases from 11 to 295 K. Interestingly, the 225-nm band occurs in all

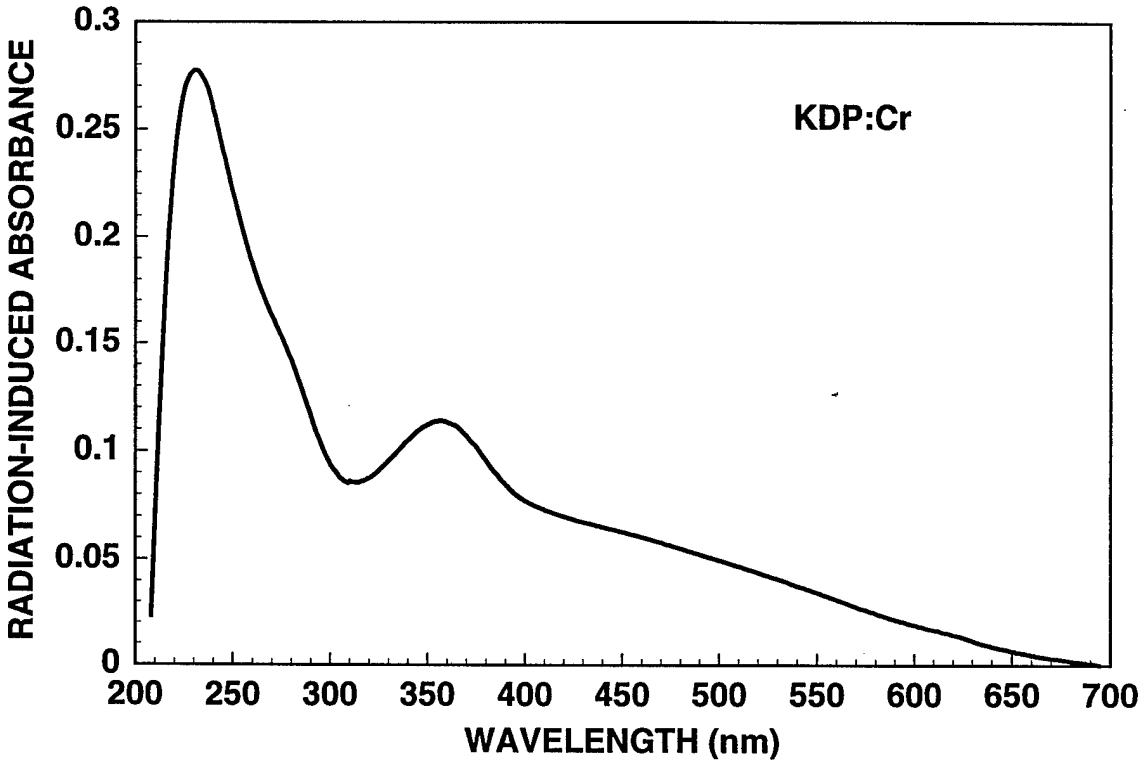

Fig. 5. Radiation-induced absorption of KDP:Cr measured at 11 K.

specimens and is therefore independent of the type of metal dopant, similar in this respect to the 275-nm band in unirradiated samples. However, the intensity of the 225-nm band decreases with the addition of metal impurities, whereas the 275-nm band in unirradiated samples increases with the addition of metal impurities. It has been suggested that the 275-nm band in as-grown crystals is associated with proton vacancies, but the defect responsible for the 225-nm absorption has yet to be identified.

The radiation-induced absorption of KDP:Cr (see Fig. 5) exhibits, in addition to the 225-nm peak, peaks near 285 and 360 nm. KDP:Fe (see Fig. 6) also exhibits peaks near 290 and 350 nm with a broad absorption maximum near 450 nm. (Note: the offset at 310 nm in Fig. 6 is an instrumental artifact associated with a change of the spectrophotometer light source.) Notice that the radiation-induced absorption in the metal-doped samples is considerably less than in the high purity specimen. To gain a better understanding of the radiation-induced defects in the KDP samples we investigated their thermal evolution.

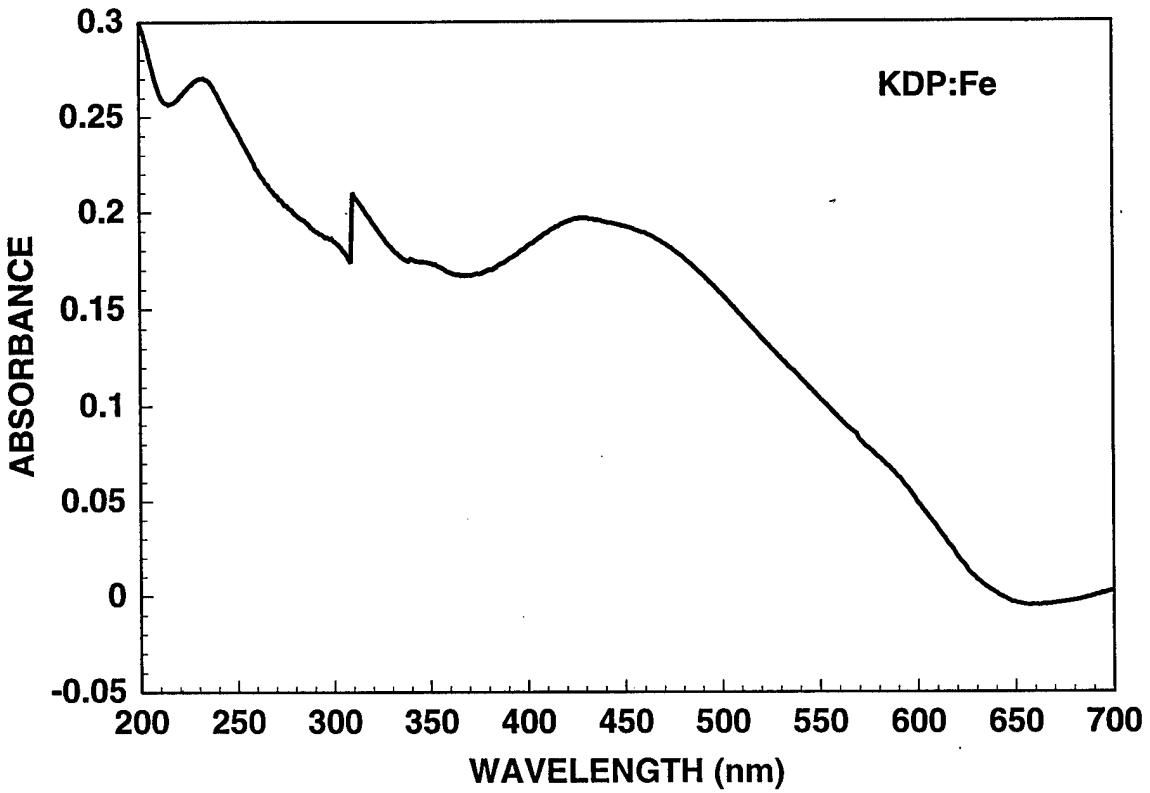

Fig. 6. Radiation-induced absorption of KDP:Fe measured at 11 K.

Shown in Fig. 7 are representative absorption spectra of the high purity sample as a function of annealing temperature. As the temperature is raised from 11 to 50 K there is considerable reduction in the intensity of the 375- and 550-nm bands whereas the 225-nm band, although broadened, is not diminished in intensity. At 100 K the individual bands are not resolved but the overall absorption is still large relative to the unirradiated absorption (295 K curve of Fig. 7). The majority of the radiation-induced absorption has thermally decayed by 150 K. Very similar behavior is observed for KDP:Al as shown in Fig. 8.

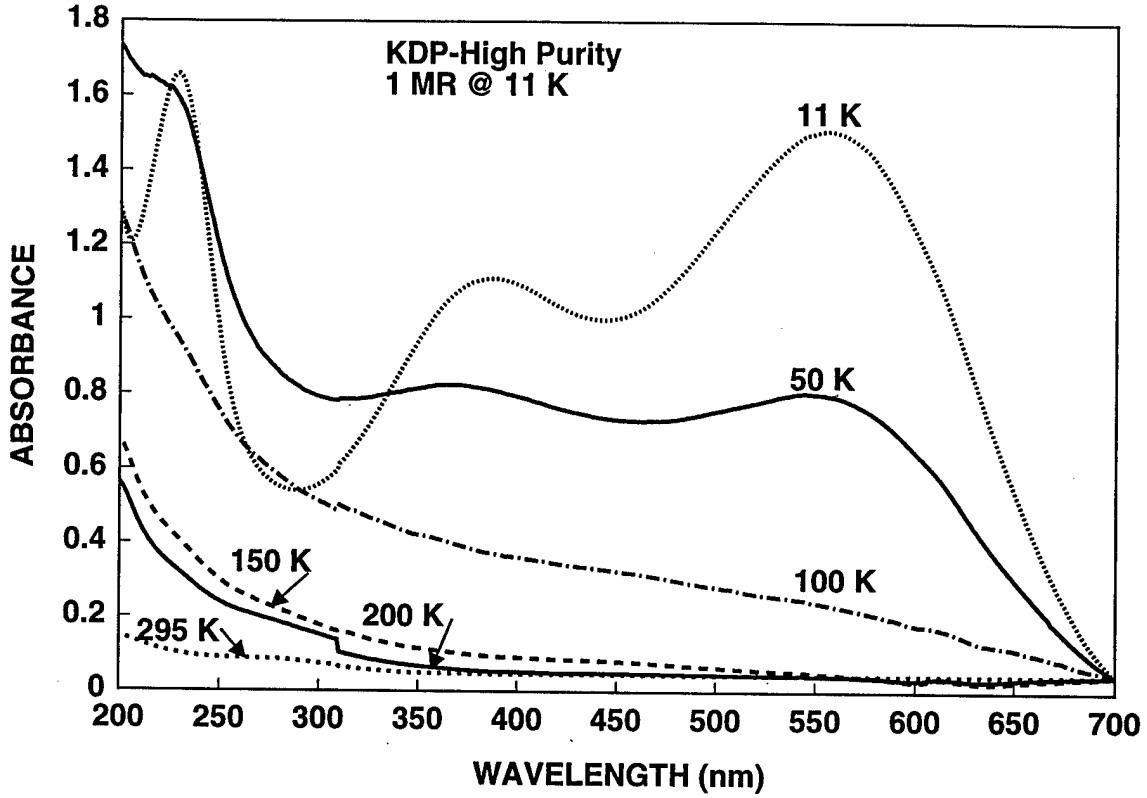

Fig. 7. Temperature-dependent optical absorption of irradiated high-purity KDP.

The temperature-dependent optical absorption of irradiated KDP:Cr is shown in Fig. 9. From the difference spectra of Fig. 5 we know that radiation-induced peaks occur at 225 and 360 nm with a knee near 285 nm. Relative to the high purity and Al-doped KDP samples, the overall magnitude of radiation induced absorption in KDP:Cr is very small. Surprisingly, there is a slight increase in the magnitude of absorption as the temperature is raised from 11 to 100 K. Notice that the radiation-induced peak at 360 nm thermally decays between 250 and 295 K. A more careful analysis of the temperature evolution of these peaks should be done by converting the spectra to energy units, and fitting with appropriate distribution functions (Gaussian, Lorentzian or Voigt). From the fitted data one could extract the area under the individual radiation-induced peaks as a function of temperature. This would yield a better data set that could be compared with the temperature dependence of the RL intensity and thermal decay of electron spin resonance signals (if any). Time constraints of the current project preclude this option.

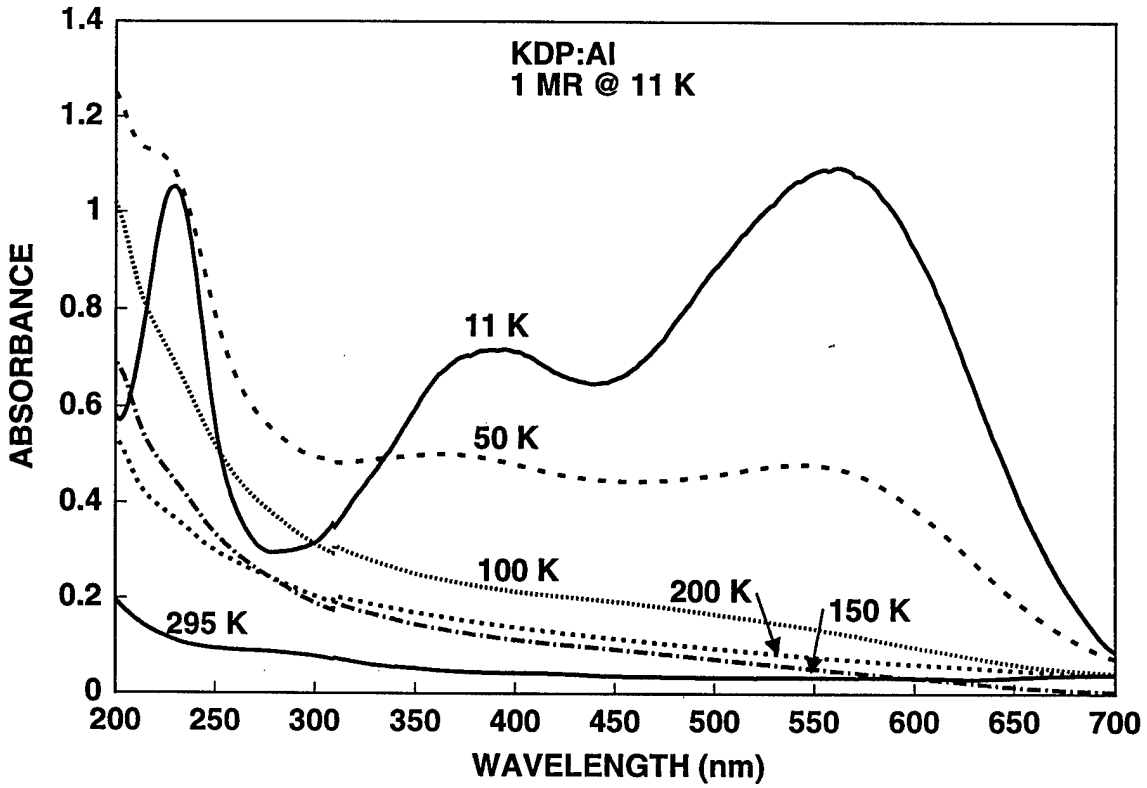

Fig. 8. Temperature-dependent optical absorption of irradiated KDP:Al.

The temperature-dependent optical absorption of KDP:Fe is shown in Fig. 10. Maxima occur near 225, 290 and 350 nm (this is better seen in the difference spectra of Fig. 6), and broad absorption extends from 400 to 650 nm with maximum near 420-450 nm. The radiation-induced absorption is reduced significantly as the temperature increases from 11 to 50 K; however, it does not thermally anneal until the temperature is above 200 K. In fact, there is strong absorption at 225 and 290 nm even at 200 K. It appears from the data of Fig. 10 that concomitant with the thermal decay of the 225- and 290-nm peaks is growth of an absorption band whose maximum lies below 200 nm. This was also observed in the behavior of the 225-nm peaks of both high purity and Al-doped KDP (see Figs 7 and 8).

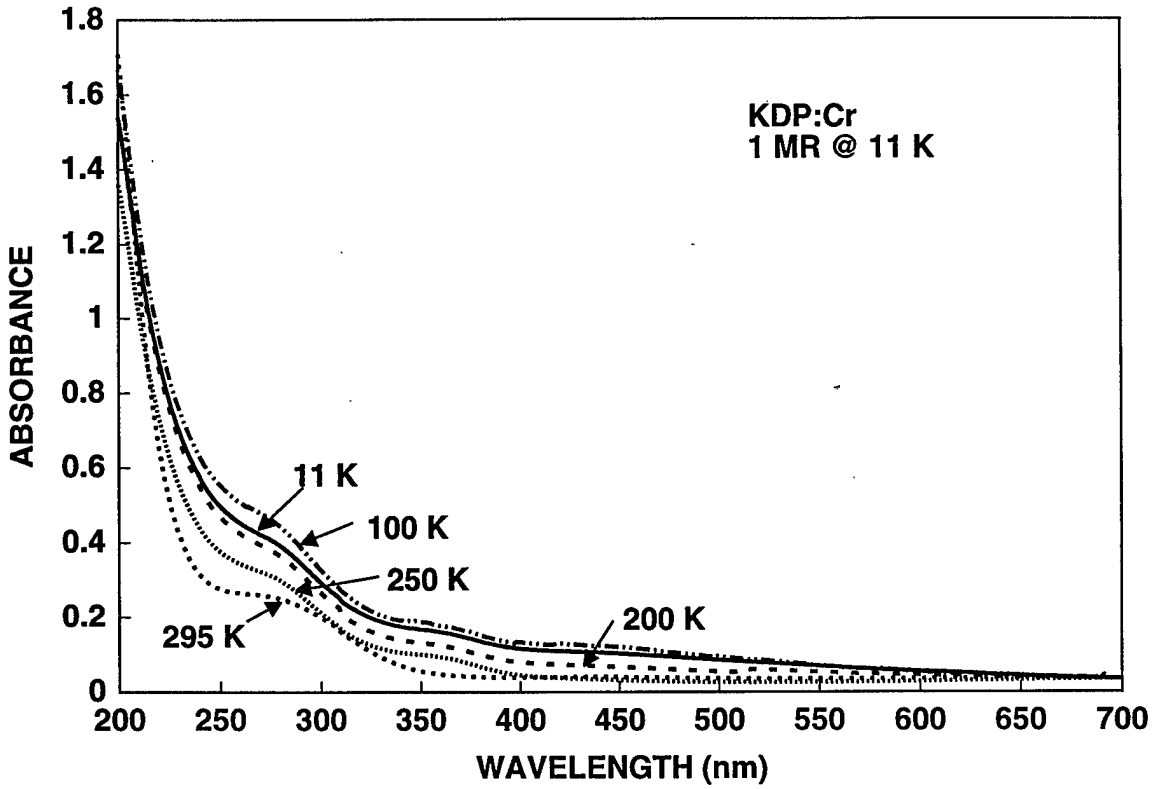

Fig. 9. Temperature-dependent optical absorption of irradiated KDP:Cr.

Recall that the transient optical absorption of KDP measured at room temperature by Davis *et al.* exhibited a very broad spectrum extending from the near-IR to the *uv*. The polarized spectrum of optically generated defects in KDP taken approximately 1 ms after 5 ns *uv* excitation ($\approx$ 0.25 GW/cm^2) at 266 nm exhibited peaks centered near 390-410 nm and 510-550 nm. The π-polarized spectrum consisted of only the 510-550 nm peak whereas the σ-polarized spectrum contained both peaks. Davis *et al.* concluded that at room temperature both the σ and π absorption spectra were due solely to defect A, contrary to the earlier work of Dieguez *et al.* [*J. Chem. Phys.* **81**, 3369 (1984)] whereby it was suggested that the σ spectrum was attributable to defect B and the π spectrum was due to defect A. The remarkable similarity between the room temperature transient absorption spectrum and the *x*-ray induced spectrum of Dieguez *et al.* observed at 10 K was noted.

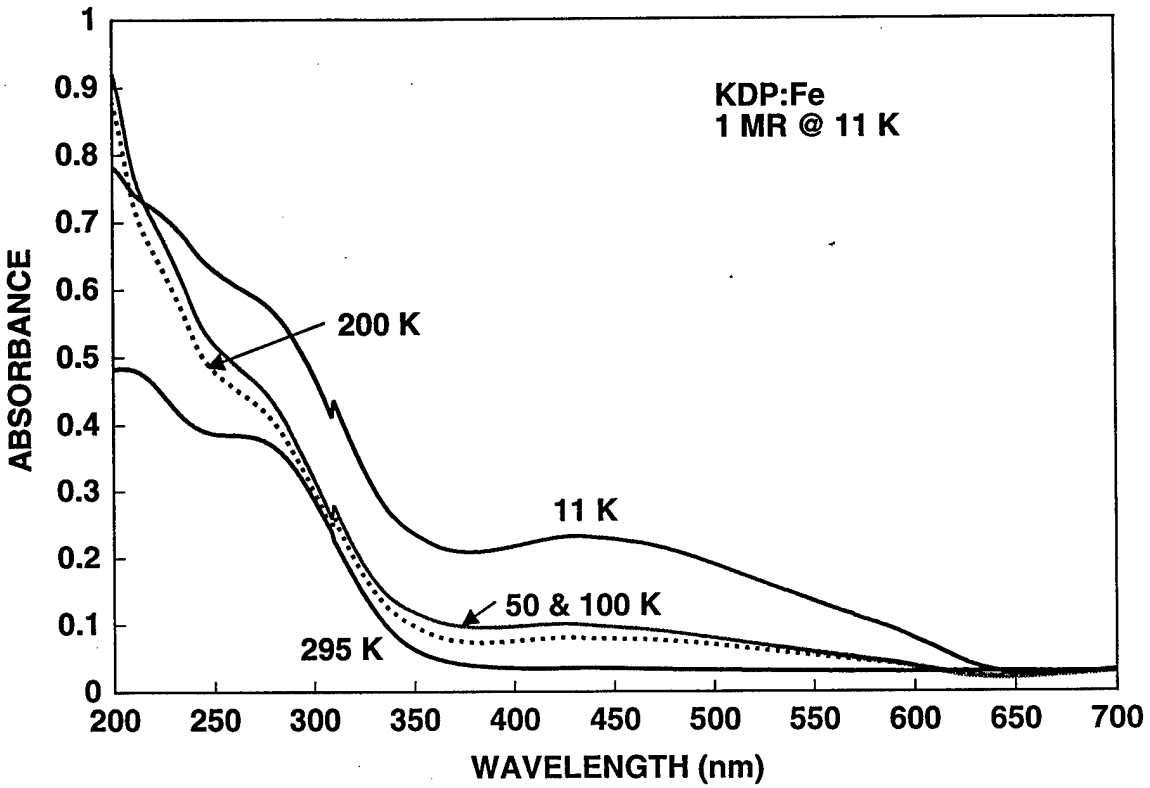

Fig. 10. Temperature-dependent optical absorption of irradiated KDP:Fe.

As depicted in Figs 3 and 4, *x* irradiation at 11 K indeed induces broad absorption with maxima near 385 and 550 nm in both pure and Al-doped KDP. In addition there is a very strong radiation-induced absorption band with maximum near 225 nm. In fact this band is induced in each of the four samples (see also Figs 5 and 6) and appears, therefore, to be intrinsic. The broad absorption above 300 nm shows variations as the metal impurity is varied, although each spectrum (Figs. 3, 4, 5, and 6) is characterized by a peak in the region 350 to 385 nm. Also we note the very strong absorption in the pure and Al-doped specimens compared to the Fe- and Cr-doped samples. We consider first the effect of irradiation on the high-purity sample. It is the general consensus that defects A and B are produced by the following reactions:

$$H_2PO_4^- \rightarrow HPO_4^{\bullet -} + H^\circ \qquad \text{(Defect A)} \qquad (1)$$

$$H_2PO_4^- + h^+ \rightarrow H_2PO^{\bullet}_4 \qquad \text{(Defect B)} \qquad (2)$$

In reaction (1) radiation breaks the relatively weak O–H bond of $H_2PO_4^-$ thereby forming $(HPO_4)^{2-}$ ("proton vacancy") and a proton. $(HPO_4)^{2-}$ stabilizes a hole and forms paramagnetic $HPO^{\bullet}_4^-$ and the proton captures an electron to form a hydrogen atom. Defect B forms when $H_2PO_4^-$ (self) traps a hole producing paramagnetic $H_2PO^{\bullet}_4$. Of course for charge neutrality there must be an equal number of trapped electrons and holes.

We note that the magnitude of radiation-induced absorption decreases in the order: high purity, Al, Cr, and Fe. This is somewhat surprising because it is usually found that impurities and defects increase the radiation-induced absorption of materials. As stated earlier the difference that can be expected in concentration of defects in the pure and M-doped samples arises due to charge compensation of the trivalent M ion. M^{3+} ions substituting for K^+ ions requires two proton vacancies for each M^{3+} ion incorporated into the sample. Also, the M ions should be a source for electrons and holes. Assuming that they enter as trivalent ions during irradiation we have the following possible reactions:

$$M^{3+} \rightarrow M^{4+} + e^- \qquad (3)$$

$$M^{3+} \rightarrow M^{2+} + h^+ \qquad (4)$$

Thus presence of the M ions may enhance the probability of the back reactions (1) and (2) during irradiation. That is,

$$H^\circ \rightarrow H^+ + e^- \qquad (5)$$

$$H^+ + HPO^{\bullet}_4^- \rightarrow H_2PO_4^- \qquad (6)$$

$$H_2PO^{\bullet}_4 + e^- \rightarrow H_2PO_4^- \qquad (7)$$

$$(HPO4)^{2-} + H+ \rightarrow H_2PO_4^- \qquad (8)$$

The inverse of reactions (3) and (4) will also occur. Assuming the radiation-induced absorption bands in the M-doped samples are associated with the previously identified defects, *viz.*, defect A, which consists of a hole center and hydrogen atom, and defect B,

consisting of a hole center, we conclude that following irradiation the concentration of these defects is less than in the pure sample perhaps due to the rich supply of electrons and holes available through metal ionization.

Additional detailed work on the temperature dependence of the absorption spectra, combined with other experimental data (RL and ESR, for example), should provide stronger evidence for the correct elucidation of the defect structure. For example, all temperature-dependent absorption data should be taken by isochronal annealing. That is, the sample under investigation should be warmed to a specific temperature for a fixed period of time and then cooled to 11 K for measurement. This is important because of the orthorhombic-to-tetragonal phase transition that occurs near 123°C in pure KDP. Visual inspection of pure KDP for T<123°C revealed the presence of grain boundaries (not observed in the tetragonal phase) that caused increased inhomogeneous scattering, which manifests itself (incorrectly in our experiments) as increased absorption. The magnitude of this effect may be small (< 10%), but should be properly considered when plotting temperature-dependent absorption band intensities. Nevertheless, the present data clearly reveal several important features. First, all four samples reveal the presence of a well-defined radiation-induced band near 225 nm that decays slowly with temperature. This band is observable even at room temperature and appears to be independent of the metal dopant. Secondly, each sample exhibits a band near 350 nm that also seems to be independent of the impurity dopant. This band decays rapidly with increasing temperature and is only weakly evident above approximately 100 K. The broad absorption in the 500 nm region also decays rapidly with temperature and appears to be altered by the metal impurity. The temperature-dependence of the peak absorption in high-purity KDP is shown in Fig. 11.

The present data are similar to optical absorption data previously presented by Dieguez and Cabrera [*J. Phys. D* **14**, 91 (1981)] with some notable exceptions. They found two overlapping bands centered at 215 and 280 nm in their nominally pure unirradiated KDP crystals, whereas we observe only the intrinsic band at 275 nm in all specimens except the Fe-doped sample, which does indeed exhibit the 215-nm band. The differences may be associated with the quality and impurity content of each sample. Upon *x* irradiating at 13 K they found two, broad, induced absorption bands in nominally pure KDP, a relatively strong one centered near 550 nm and a weaker one centered near 390 nm.

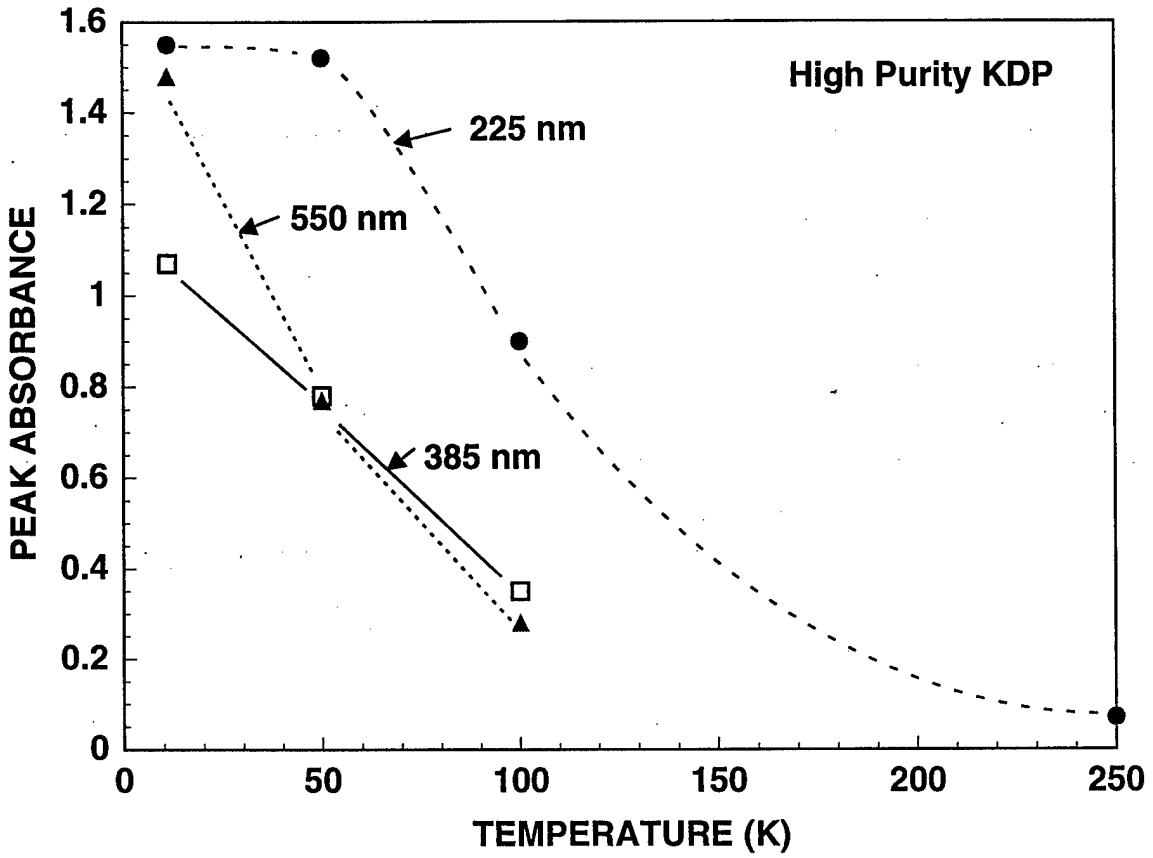

Fig. 11. Temperature dependence of the radiation-induced peak absorption in high-purity KDP.

These are similar to our 375- and 550-nm bands and we assume they arise from the same radiation-induced defect(s). Dieguez and Cabrera noted that upon irradiation the intrinsic 215- and 285-nm bands were modified in a complicated way and chose not to study them further. Our results show a very prominent radiation-induced band at 225 nm that does not appear to be a modification of the intrinsic 275-nm absorption. Because the temperature-dependent RL emission provides additional information on point defects in KDP, and may be related to the radiation-induced optical absorption bands, we opt to present the RL results before delving into a discussion of possible defects associated with the three main absorption bands.

B. Radioluminescence

Shown in Fig. 12 are the RL spectra for high-purity KDP taken as a function of temperature. The dominant emission is a band centered near 490 nm that decays rapidly with increasing temperature. At 80 K the main emission band is undetectable and a weak band appears near 350 nm. This latter band is still evident at 300 K and is clearly seen as second order emission near 700-750 nm. Use of a cutoff filter that transmits all wavelengths above but not below 400 nm was used to establish that the 700-nm emission is second-order emission of the 350-nm band. Similar spectra are observed in KDP:Al as shown in Fig. 13. Again the 490-nm emission decays rapidly with temperature, but unlike the high-purity emission there is significant growth of the 350-nm band. In fact at 80 K the intensity of this band is greater than the intensity of the 490-nm band measured at 7 K. This band exhibits a significant reduction in intensity as the temperature increases from 80 to 120 K. However, there is still measurable emission even at 300 K (not shown).

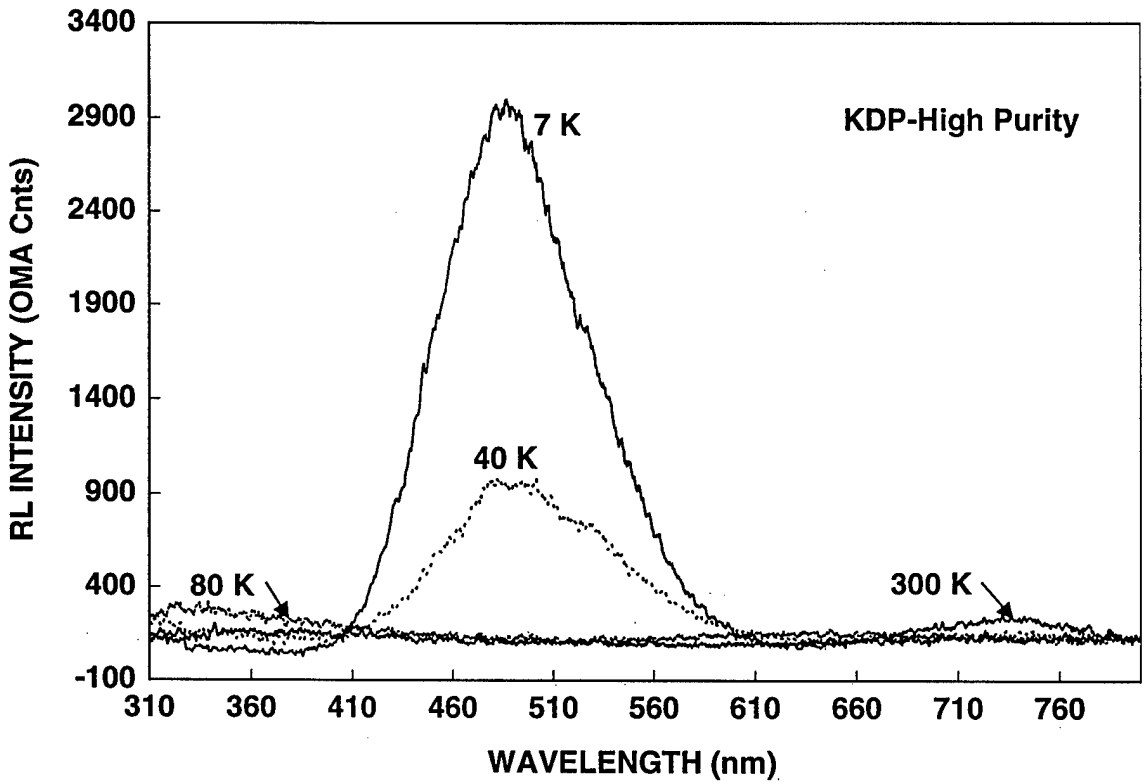

Fig. 12. Temperature-dependent RL emission from high-purity KDP.

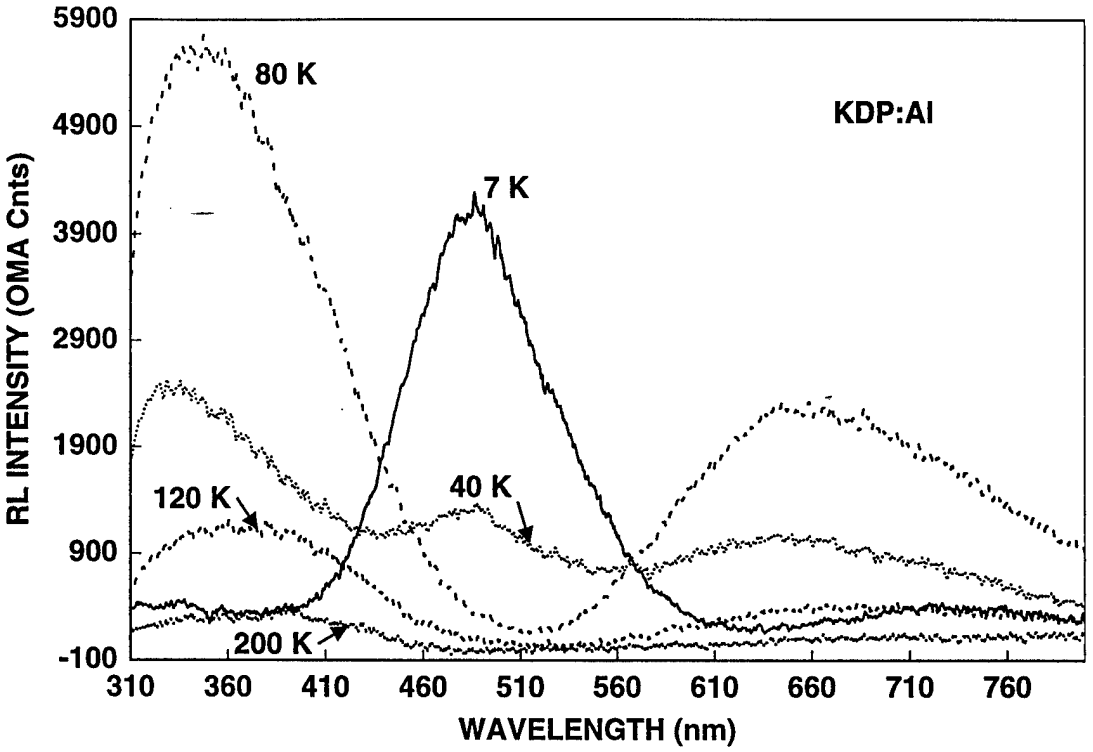

Fig. 13. Temperature-dependent RL emission from KDP:Al.

Figure 14 depicts the temperature-dependent RL emission from KDP:Fe. Interestingly, there is evidence of an emission band below 300 nm at 7 K which was not observed in any other sample. The usual strong emission occurs near 490 nm and rapidly decays with increasing temperature. At 80 K there is no measurable emission at 490 nm, but there is evidence of a very broad emission that spans the region from 300 to 460 nm. As the temperature increases to 120 K the broad emission collapses into a single emission band with maximum near 410 nm. This band is essentially constant in intensity and peak position up to 300 K.

From the collective RL data we note that the main emission near 490 nm occurs in each specimen and is therefore independent of the metal impurity. The question arises as to whether this intrinsic emission is correlated with either the 225- or 385-nm absorption bands that also appear to be intrinsic. Recall that the 550-nm absorption band was altered by the addition of metal impurities. From Fig. 11 we see that the 225-nm band in pure KDP decays slowly with temperature whereas the RL emission decays by 80 K. This suggests that either the 490-nm emission is unrelated to the 225-nm band, or it is related

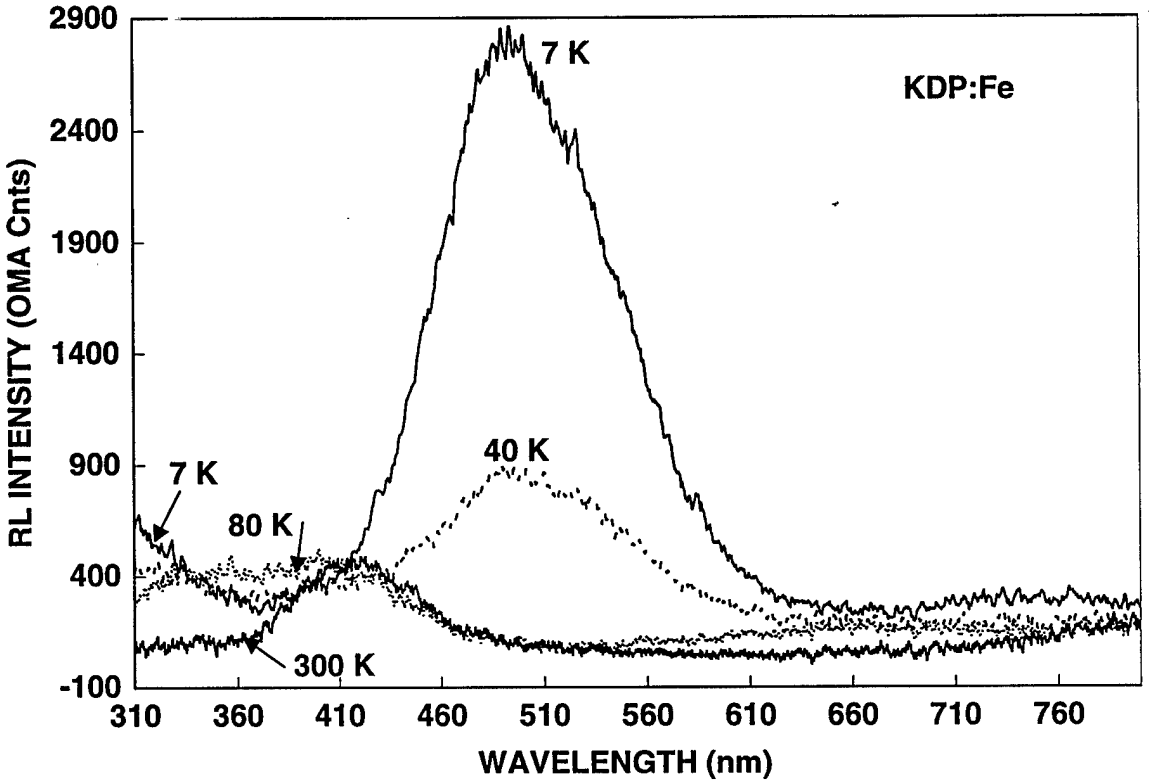

Fig. 14. Temperature-dependent RL emission from KDP:Fe.

but the RL *radiative* recombination rate is a strong function of temperature such that above about 80 K the recombination is dominated by *nonradiative* processes. A comparison of the individual absorption peak intensities *vs T* (Fig. 15) and the RL emission in KDP:Al (see Fig. 13) strongly suggests, however, that the 225-nm absorption is not associated with the 490-nm emission. The RL emission of Fig. 13 shows a precipitous drop in intensity between 7 and 40 K, whereas the 225-nm absorption peak actually increases in this temperature interval. In fact it is the 350-nm emission that mimics the temperature dependent behavior of the 225-nm absorption. This is true for each of the four KDP samples. Therefore, *we speculate that the 225-nm absorption observed in each KDP specimen is associated with the 350-nm RL emission.* The intensity of this emission is

dependent upon both impurity and temperature, similar to the behavior observed from the radiation-induced 225-nm absorption band.

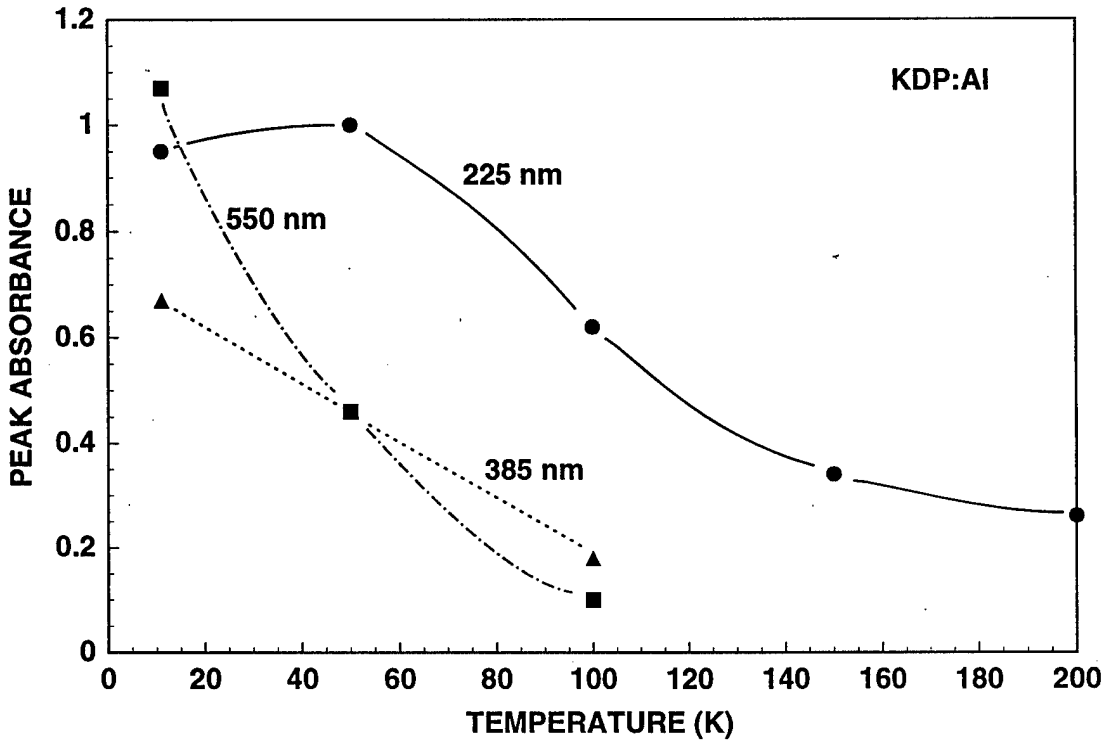

Fig. 15. Temperature dependence of the radiation-induced peak absorption in high-purity KDP:Al

The RL data also show that each specimen exhibits weak emission in the 350 to 400 nm region that, as discussed above, is dependent upon temperature and impurity. As seen most clearly in Fig. 14, this emission comprises more than one band that evolves with temperature. Note the broad absorption in this region for $T = 80$ K and the narrower band that occurs for $T \geq 120$ K. Notice also the clear indication of an emission band with maximum below 310 nm at $T = 7$ K. This is consistent with data of Dieguez *et al.* [*J. Chem. Phys.* **81**, 3369 (1984)] wherein they reported an RL peak near 260 nm. These data suggest a complex evolution with temperature that also depends upon metal impurity.

The main RL emission band (490 nm) decays rapidly in the temperature interval 7 to 80 - 100 K, which is also the region of rapid thermal decay for both the 385- and 550-nm absorption bands. We can rule out any correlation of this emission with the 550-nm absorption for two reasons. First, in the absence of an unknown energy transfer

mechanism, the emission energy cannot exceed the absorption energy. Secondly, the 550-nm absorption has been shown to be impurity dependent, unlike the 385-nm absorption and 490-nm emission. This suggests that *if any correlation exists between the 490-nm RL emission and absorption it is with the 385-nm band.*

Dieguez *et al.* [*ibid.*] observed a 485-nm RL band from their KDP and KD*P samples when the irradiation temperature was less than 80 K; in addition, for irradiation temperatures greater than 80 K a new emission band appeared at 350 nm. It was noted that this band, which occurred in both KDP and KD*P, reached maximum efficiency at T_c, thus suggesting that the luminescence mechanism was related to the behavior of the hydrogen sublattice. This behavior is observed in some but not all of our KDP samples. Most notably in KDP:Al (Fig. 13) we observe maximum RL emission intensity at 80 K and significantly diminished intensity at $T = 120$ K.

Comparing now the RL and optical absorption behavior, along with previously identified defects, we can draw some preliminary conclusions regarding the point defects in KDP. The 225-nm radiation-induced optical absorption band occurs in each sample, independent of impurity dopant, and decays slowly in the interval 50 - 200 K (see Figs. 11 and 15). This is the same temperature interval in which defect A [Reaction (1)] thermally decays. And although the RL emission near 350 nm is complex, its general temperature behavior suggests that it may be correlated with the 225-nm absorption. Thus we tentatively suggest that the 225-nm absorption band is due to the $HPO_4^{\bullet -}$ radical ion. Additional work should be undertaken to see if hydrogen atom absorption occurs below 200 nm. The radiation-induced optical absorption data clearly indicate the presence of a band below 200 nm (see Fig. 7, for example).

Radiation-induced optical absorption at 385 nm decays rapidly as temperature increases from 11 to near 100 K, although there is still very weak absorption up to 300 K in the impurity-doped samples. Defect B [Reaction (2)] has been shown to decay rapidly in this same temperature interval, and ESR measurements show that it cannot be induced by irradiation at 77 K. This is similar to the behavior of the 490-nm RL emission and we suggest that 385-nm absorption is associated with defect B. Our present data are insufficient to allow identification of the defect associated with the 550-nm absorption band. We failed to observe any RL emission up to 800 nm that could be associated with this band.

Finally, we discuss our results in conjunction with the seminal work of Dieguez *et al.* and Davis *et al.* Optical absorption in KDP was investigated by Dieguez *et al.* following *x* irradiation at 10 K, whereas Davis *et al.* measured the *transient* optical absorption induced at room temperature by 266-nm photon excitation. Dieguez *et al.*

measured the polarized absorption and found the π-spectrum to consist of a broad band with maximum at 510 nm; this absorption was assigned to defect A. The σ-spectrum consisted of broad absorption with maxima at 390 and 550 nm, and was attributed to defect B. Davis *et al.* measured similar polarized absorption in KDP, finding the σ-spectrum to consist of two peaks near 390-410 and 510-550 nm, and the π-spectrum characterized by maximum near 510-550 nm. The similarity of the *x*-ray induced absorption spectrum with the transient one measured by Davis *et al.*, led the latter to suggest that the same defects were likely responsible for the absorption spectra. However, Davis *et al.* concluded that the σ and π room temperature absorption spectra were due to only defect A. But, at low temperatures ($T \leq 77$ K) the π-spectrum was due primarily to defect A whereas the σ-spectrum was due to both defects A and B.

Our present data suggest that defect B is associated with 385-nm absorption. This defect center decays rapidly between 11 and 100 K, but is still evident at room temperature, especially in the metal-doped specimens. Under intense *uv* excitation at room temperature it is likely that this center is observed in the experiments of Davis *et al.* Further, our results suggest that defect A is not associated with either 385- or 550-nm absorption, but is attributable to 225-nm absorption. We offer no identification of the 550-nm absorption but note that it is dependent on the metal dopants in KDP.

4. CONCLUSIONS

Investigation of point defects in KDP by temperature-dependent optical absorption and RL measurements reveal the presence of at least three defects with strong evidence for the existence of others. Distinguishable absorption bands occur at 225, 385 and 550 nm in KDP following *x*-ray excitation at 11 K. From the temperature behavior of these bands, in conjunction with previous experimental data, we suggest that the bands are attributable to defect A, defect B, and an unknown impurity related center, respectively. These results are not in agreement with the conclusions of either Dieguez *et al.*, or Davis *et al.*

For NIF applications there are several observations that merit discussion. First, there is a strong radiation-induced optical absorption band at 225 nm that persists even at room temperature in pure and metal-doped KDP. This band must be accounted for when considering any 4ω application. Pure KDP at low temperatures (~ 11 K) is much less radiation hard than any of the metal-doped samples; however, at room temperature the pure sample exhibits the least absorption. No *x*-ray-induced absorption occurs at room temperature, but the metal-doped samples show enhanced absorption relative to pure KDP owing to an intrinsic band at 275 nm associated with proton vacancies. The principal RL emission bands at 350 and 490 nm decay rapidly with increasing temperature so that at

room temperature there is no evidence for 490-nm emission and only weak emission at 350 nm. The strongest emission recorded at room temperature of any KDP sample investigated occurred in KDP:Fe, the maximum being centered near 410 nm. Thus, although there is measurable absorption in many of the KDP samples at room temperature, there is only very weak emission. This may explain why Yan *et al.* [M. Yan, M. Staggs, M. Runkel and J. De Yoreo, LLNL preprint] failed to observe emission other than blackbody radiation during laser photoexcitation of KDP.

The complexity of the temperature-dependent absorption and emission of KDP demands a more careful study than has been previously conducted. Absorption and emission spectra, taken over much smaller temperature intervals (~ 10 K) than was done in the present work, must be recorded and fitted with know spectral functions thus allowing more accurate plots of intensity *vs.* temperature, for example. A more detailed investigation of the complex optical absorption occurring below 400 nm must be undertaken to sort out the contributions of various defects. Concomitant with the optical work must be similar temperature-dependent ESR studies to assist in elucidating the point defects in KDP.

Report Number (14) LA-UR--97-4967

Publ. Date (11) 199710

Sponsor Code (18) DOE/MA, XF

UC Category (19) UC-901, DOE/ER

DOE